Agromet 37 (1): 54-65, 2023

Agromet
journal.ipb.ac.id/index.php/agromet
ISSN : 0126 - 3633

Sea Surface Temperature Anomaly Characteristics Affecting Rainfall in Western Java, Indonesia

Qurrata A'yun Kartika[1,2], Akhmad Faqih[1], I Putu Santikayasa[1], Amsari Mudzakir Setiawan[2]

[1]Department of Geophysics and Meteorology, Faculty of Mathematics and Natural Sciences, IPB University, Dramaga Campus, Bogor, Indonesia 16680

[2]Indonesia Agency for Meteorology, Climatology, and Geophysics, Jakarta, Indonesia

ARTICLE INFO

Received
13 October 2022

Revised
02 April 2023

Accepted for Publication
11 May 2023

Published
30 June 2023

doi: 10.29244/j.agromet.37.1.54-65

Correspondence:
Akhmad Faqih
Department of Geophysics and Meteorology, IPB University, Indonesia
Email: akhmadfa@apps.ipb.ac.id

This is an open-access article distributed under the CC BY License.
© 2023 The Authors. *Agromet.*

ABSTRACT

Western Java is densely populated with high socio-economic activity. Climate-related disasters can be mitigated with the support of an understanding of systems that produce reliable climate predictions. One of the climate variables included in hydrometeorological disasters is rainfall. The characteristics of rainfall in Western Java cannot be separated from the sea surface temperature (SST) around the area. This study compares the relationship between SST and rainfall with singular value decomposition (SVD) and compares it with Pearson's correlation. SVD Model performance was evaluated using square covariance fraction (SCF) and Pearson correlation. The results showed that rainfall has a higher correlation with SST Anomaly (SSTA) by using SVD, with a correlation of about 0.63 in 6 to 9 months without lag time. Rainfall in western Java was closely related to the positive SSTA anomaly in southern Indonesia, especially the waters south of Java Island, and negative anomalies in other areas. Furthermore, atmospheric dynamic analysis showed that the positive coefficient expansion is followed by warmer SST, lower surface air pressure, higher water vapor, and higher rainfall, all were respective to their normal conditions around western Java. This study concludes that warmer SSTA around Western Java causes increased rainfall in western Java than normal and potentially impacts the hydrological disaster in West Java.

KEYWORDS

anomaly, rainfall prediction, rainfall singular value decomposition, sea surface temperature, square covariance fraction

INTRODUCTION

Indonesia is the country with the fourth highest population in the world with the most concentrated population in Java Island. The country is also inseparable from climate-related disasters, especially hydrometeorological disasters which account for 99% of all-natural disasters (Avia, 2019; Jati et al., 2019; Wuryanta, 2022) which pose a significant threat to numerous lives. Western Java, encompassing Banten, DKI Jakarta, and West Java provinces excels in agriculture, forestry, fisheries, industry, trade, and other sectors. Being adjacent to the capital city, Banten and West Java provinces play a crucial role in supporting governmental, logistical, and industrial activities in DKI Jakarta Province, catering to the country's diverse needs. These activities, however, face frequent impacts from hydrometeorological disasters associated with abnormal and extreme rainfall patterns. Consequently, providing precise rainfall predictions at various time scales becomes vital in minimizing losses and damages caused by various climate-related disasters within the meteorological sciences and atmospheric science framework.

Indonesia experiences three primary types of rainfall, namely monsoon, equatorial, and local precipitation (Aldrian and Susanto, 2003; Lee, 2015; Lee et al., 2022). These rainfall patterns are influenced by

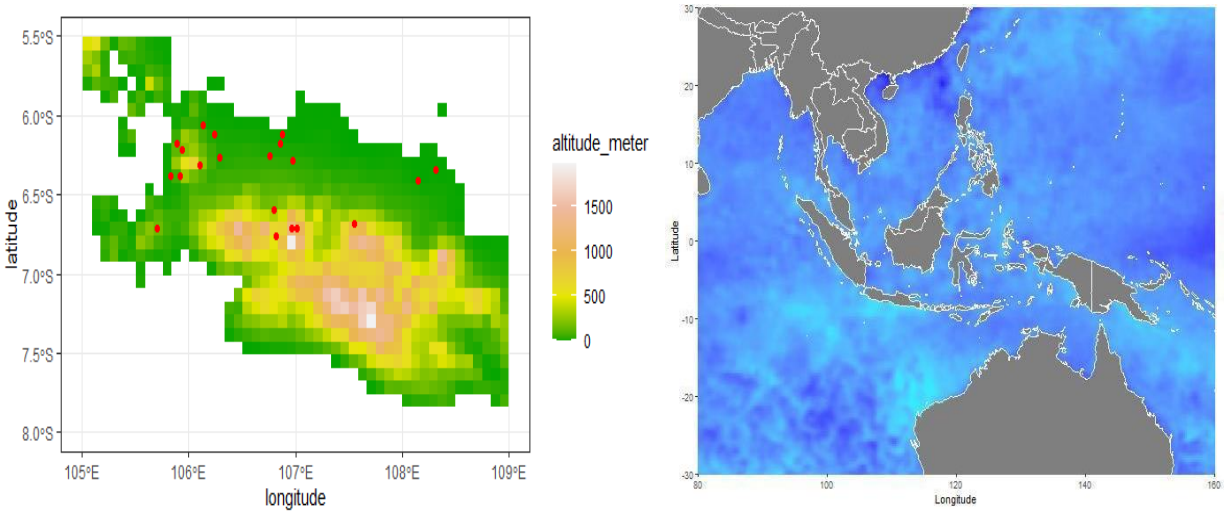

Figure 1. The location of: (a) rain gauge stations in western java for the study, and (b) the domain of sea surface temperature (SST).

various physical mechanisms that impact their variability. The process of rainfall begins with the absorption of energy by the Earth, particularly in the ocean, leading to the abundant release of water vapor into the atmosphere. Subsequently, this water vapor condenses to form clouds, which have the potential to generate rainfall. Some studies have identified sea surface temperature (SST) as a significant factor in predicting evaporation and rainfall (Aldrian and Susanto, 2003; Supari et al., 2018). It is because warm SST promotes surface turbulence, increasing air humidity and facilitating convection. These conditions cause the interaction of the sea and the atmosphere (Oueslati and Bellon, 2015). SST exhibits a positive feedback mechanism for the SST-rainfall relationship, representing sea-atmosphere interactions that can occur with or without lag times (Biasutti, 2019; Ivanova et al., 2021; Izumo et al., 2020). SST anomalies can significantly influence rainfall patterns and contribute to extreme weather conditions. In the maritime continent, such as Indonesia, SST is crucial in driving complex and extensive circulation patterns. Due to its geographical location surrounded by oceans, Indonesia is highly influenced by SST anomalies associated with various climate variabilities, such as El Niño Southern Oscillation (ENSO), Indian Ocean Dipole (IOD), Pacific Decadal Oscillation (PDO), and south pacific convergence zone (SPCZ) (Chen et al., 2019; Iskandar et al., 2019; Ivanova et al., 2021; Nguyen et al., 2021; Xu et al., 2019; Yu et al., 2021).

Numerous methods were created to assess the correlation between SST and rainfall (Aldrian and Susanto, 2003; Lee, 2015; Nurrohman and Tjasyono, 2016; Supari et al., 2018), including the use of singular value decomposition (SVD) (Ma et al., 2020). Prohaska in 1976 was the first meteorologist to use SVD analysis on surface temperature and sea level pressure (Y. Huang et al., 2021). SVD separates two related linear fields by maximizing covariance values, producing strong correspondences between two related covariance matrices such as that between SST and rainfall covariance matrices. In this case, SVD is different from PCA which comes from the statistical domain which is applied to find the main direction of the average data (Reitberger and Sauer, 2020).

RESEARCH METHODS

Study Area

This study focused in Western Java which include Banten, West Java, and Jakarta. A total 20 from the Agency for Meteorology, Climatology, and Geophysics (BMKG) stations were analyzed (Figure 1a).

Data Source

This study used 30 years of daily rainfall and SST data within 1982-2011 periods. Rainfall data of 20 stations were collected from the Agency for Meteorology, Climatology, and Geophysics (BMKG) (Figure 1a). The sea surface temperature (SST) data was used in the study was the Daily Optimum Interpolation Sea Surface Temperature data version 2.1 (DOISST v2.1) (B. Huang et al., 2021) obtained from National Oceanic and Atmospheric Administration (NOAA/NCEI), with spatial resolution of 0.25º×0.25º. DOISST v2.1 was different from the previous version (DOISST v2.0). It was updated through the addition of argo-floats as in situ data to complete the gap in the distribution of data found in DOISST v2.0mmm. This newest version was claimed to successfully reduce bias from the previous

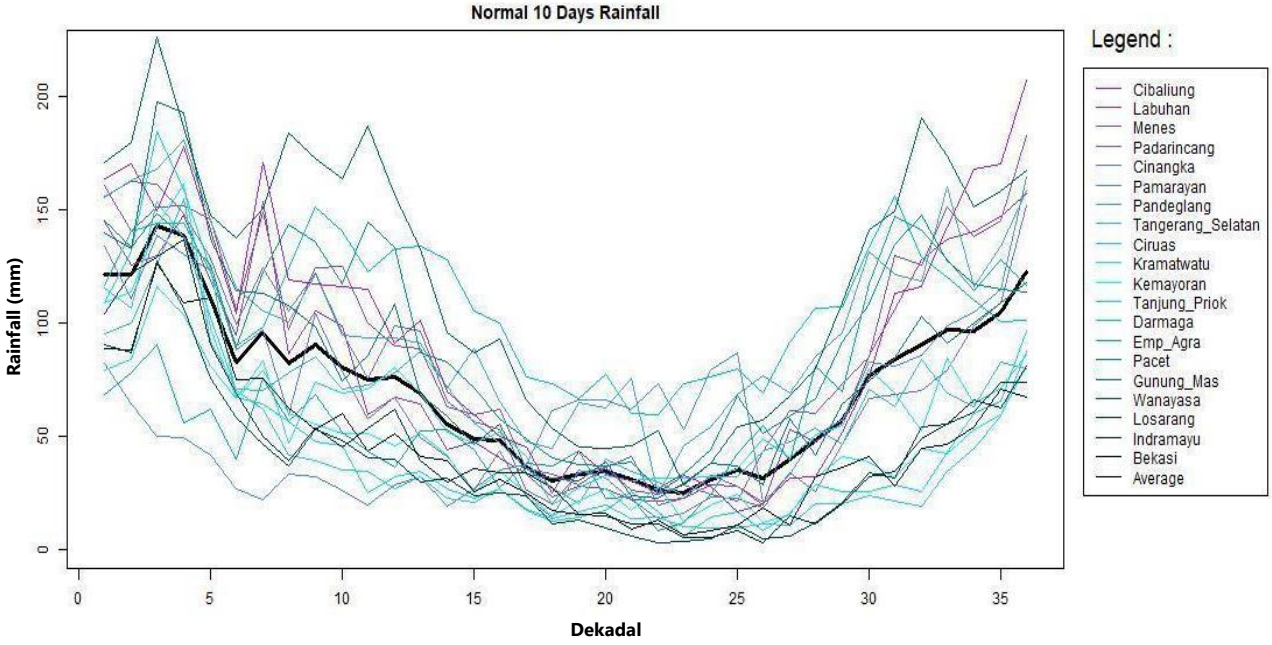

Figure 2. A dekadal rainfall (mm/10 days) for 20 stations in Western Java.

version up to 0.13ºC (B. Huang et al., 2021). DOISST v2.1 can be downloaded at https://downloads.psl.noaa.gov/Datasets/noaa.oisst.v2.highres/. SST domains were located at coordinates 80ºW to 160ºW and 30ºS to 30ºN showed in Figure 1b.

Singular Value Decomposition (SVD)

To enhance the understanding of the atmospheric dynamics that contribute to the correlation between sea surface temperature (SST) and rainfall variability, reanalysis data of surface pressure (P1000) and precipitable water content (PWC) variables were used. The data were collected from the National Centers for Environmental Prediction-Department of Energy (NCEP-DOE) dataset with a spatial resolution of 2.5º×2.5º. PWC describes the amount of water vapor contained in a column of air from the surface to the top atmosphere. The support dataset has the same domain as the SST domain.

In the realm of meteorology, precipitation data collected over consecutive 10-day periods was commonly employed to determine the onset and cessation of rainy and dry seasons (Wati et al., 2019). By utilizing this time frame, the prediction model for 10-day-scale rainfall anomalies becomes both intriguing and significant. In this particular study, the average rainfall anomaly for a specific area was utilized as a predictable factor. The reference point for normal rainfall or SST was established by calculating the average values during the period from 1982 to 2011, also on a 10-day scale. Rainfall or SST anomalies (SSTA) were defined as the differences between the actual data and the normal values, encompassing both rainfall and SST, along with their supporting variables.

This study used SVD to identify the SSTA and rainfall anomaly relationship. SVD can be used to detect pairwise patterns between climate parameters with temporal construction and one scalar variable (Reitberger and Sauer, 2020). The formula of SVD described in Equation 1.

$$\mathrm{C} = \mathrm{S}^{\mathrm{t}} \times \mathrm{P} \quad (1)$$

The covariance matrix C was the multiplication of the SSTA S matrix transpose with the rainfall matrix P. Then the covariance matrix C was decomposed using the SVD method which was denoted according to Equation 2

$$\mathrm{C} = \mathrm{ULV}^{\mathrm{t}} \quad (2)$$

U was a singular vector S (SSTA), V was a singular vector P (rainfall) and L was a diagonal matrix. The expansion coefficient concerning time or what was often also called the time exponential coefficient (TEC) SSTA was expressed by A and rainfall by B, which was obtained from Equations 3 and 4.

$$\mathrm{A} = \mathrm{SU} \quad (3)$$

$$\mathrm{B} = \mathrm{PV} \quad (4)$$

TEC can be calculated only if the values of U and V were orthogonal. The best mode for each TEC was obtained based on the square covariance fraction (SCF) with the highest percentage and was supported by Pearson correlation between TECs in each mode. The SCF value was expressed by the Equation 5.

$$SCF = \frac{{l_i}^2}{\sum {l_i}^2} \quad (5)$$

Thus, the output expansion coefficient had 2 modes, and the expansion coefficient of Mode 1 had the largest SCF value that was not explained by other modes (Bretherton, 2015; Bretherton et al., 1992). SCF describes the similarity of variations of the two variables, the greater the value of SCF, the better the simulation was considered. SVD analysis was performed with and without time lag (lag 0 to lag 4 in a duration of 10-day) to analyze the time series relationship between SSTA and rainfall. The SSTA expansion coefficient from SVD was correlated with rainfall at different time lags using Pearson correlation.

SVD pattern simulation was carried out for the SSTA expansion coefficient separately using modes 1 and 2, and a combination of modes 1 and 2 (C12). The combination of modes 1 and 2 was taken by multiple regression with rainfall anomaly as the result. The formation of rainfall anomalies by SSTA can occur in several timeframes, therefore a moving average analysis needs to be done. Moving average analysis was carried out in this study for 3, 6 and 9 months.

The description of atmospheric dynamics in relation to the characteristics of SSTA characteristics and rainfall was explained by other variables, including surface pressure and PWC. Theoretically, when the SST increases, it warms the air near the surface, causing it to expand. This expansion leads to a decrease in surface pressure, which in turn triggers the upward movement of warm air. As the warm air rises, it carries water vapor along with it. This process results in an increase in the amount of water vapor within the vertical column of air, and eventually, at a certain point, this water vapor condenses and falls as precipitation. The process described in this study was illustrated in Figure 3.

RESULTS AND DISCUSSION

Western Java typically experiences a monsoonal rainfall pattern, with peak rainy season during December, January, and February (DJF), whereas dry seasons typically peak between July, August, and September (JAS), as shown in Figure 2. The same thing was stated by Aldrian and Susanto (Aldrian and Susanto, 2003) for monsoonal type of rainfall pattern, but with the peak of the dry season being one month earlier. Generally, when it comes to the dry season, there was a consistent decrease in rainfall since the first 10 days of February in few areas such as Cibaliung, Labuhan, Menes, Padarincang, Cinangka, Pamarayan, Pandeglang, Tangerang Selatan, Kemayoran, Darmaga, Pacet, Gunung Mas and Indramayu. Ciruas, Kramatwatu, Tanjung Priok, Emp Agra, Wanayasa and Losarang have their peak rainfall in the last 10 days of January. Wanayasa has a unique rain characteristic where the average daily rainfall in the second 10 days in November to the last 10 days in May was above 15mm with a fluctuating pattern.

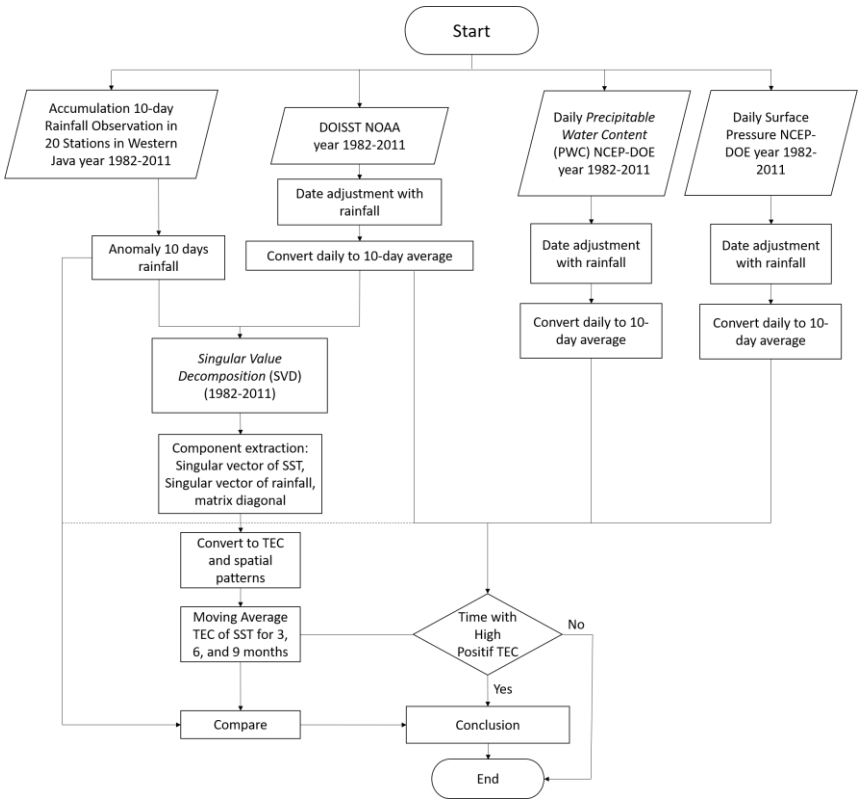

Figure 3. Flowchart of the research method to determine rainfall anomaly based on the characteristic of sea surface temperature analysis (SSTA).

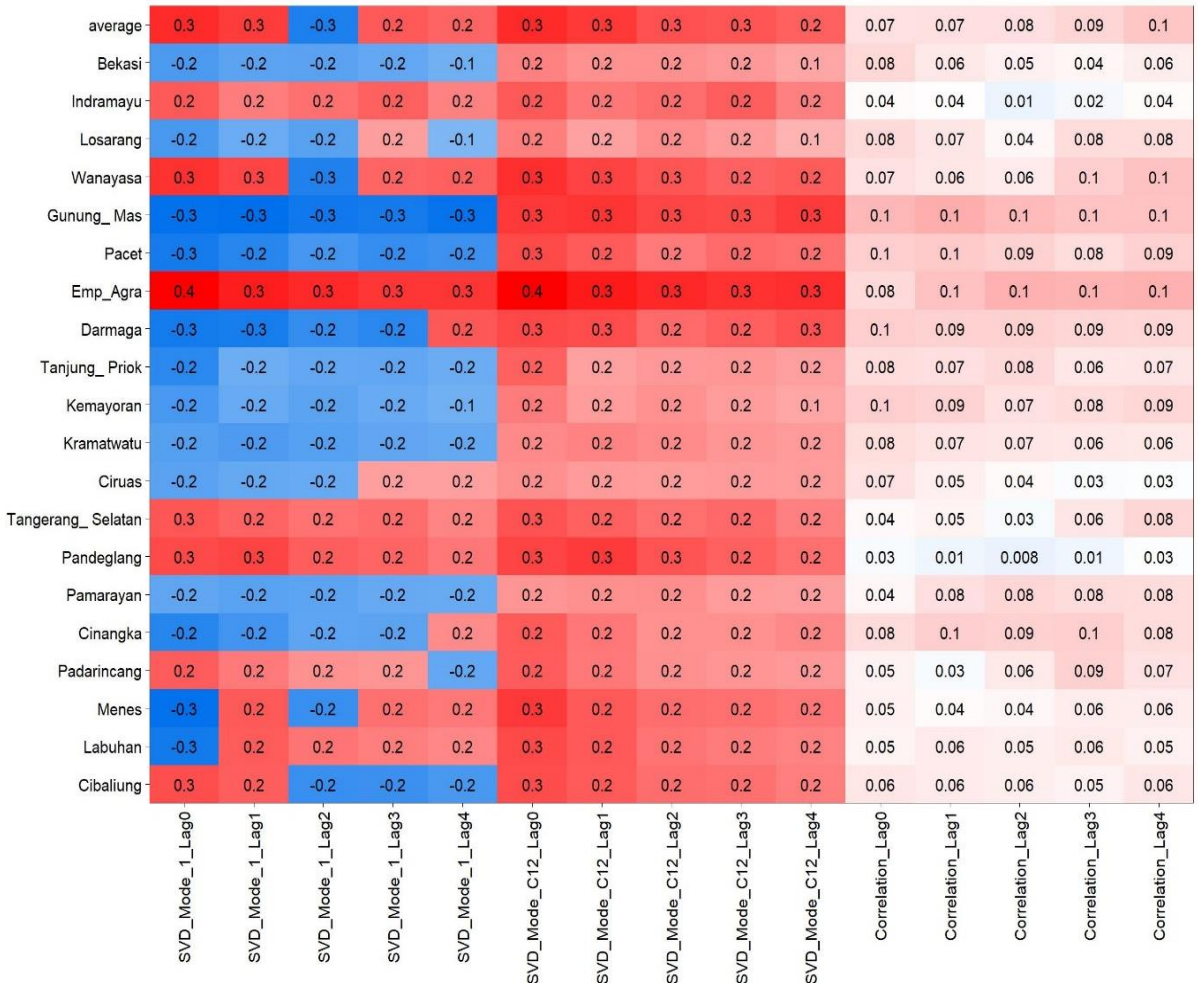

Figure 4. Singular value decomposition (SVD) expansion coefficient correlation mode 1, mode C12 with rainfall and the highest correlation of sea surface temperature (SST) grid with rainfall.

Figure A1 displays the covariance map generated from singular value decomposition (SVD) analysis of rainfall against SST Mode 1 rainfall data. (Bretherton et al., 1992), notes this similarity between covariance maps created from an SVD analysis and correlation maps. An almost constant spatial pattern of sea surface temperature anomaly (SSTA) in SVD Mode 1 depicted in Figure A1. This highlights negative anomalies across various time lags across western Indian Ocean, South China Sea and parts of Pacific Ocean regions. Conversely, positive SSTA anomalies have been observed across most Indonesian waters - this pattern indicating the existence of a pole located centered within Indonesian waters which influences all nearby regions. based on research conducted by (Makula et al., 2020), the characteristics of the SVD spatial patterns were closely related to climate phenomena which can be related to circulation, energy, and humidity caused by the oceans, and other land-generating systems. This pattern corresponds directly with Aldrian and Susanto (Aldrian and Susanto, 2003)'s findings concerning PC1 in monsoon rainfall patterns with SST accounting for 30.8% variance within it.

Figure A1 represents the distribution of correlations between the expansion coefficients of sea surface temperature anomalies (SSTA) in SVD Mode 1 and rainfall, the correlation between the expansion coefficient of SSTA in SVD Mode C12 and rainfall and the highest correlation between SSTA and rainfall. The top 50% of correlations were dispersed southward from West Java, covering areas such as Cibaliung, Labuhan, Menes, Pandeglang, South Tangerang, Darmaga, Emp_Agra, Pacet, Gunung Mas, and Wanayasa. The highest correlation for Emp_Agra at lag 0 between rainfall and expansion coefficient of SSTA in SVD Mode 1 and Mode C12 was 0.36. On the other hand, the lowest correlation for Losarang at Lag 0 between rainfall and SSTA was 0.08 (very low relationship). In general, the correlation between SSTA and rainfall tends to be lower compared to the correlation between the expansion coefficient of SSTA in SVD and rainfall. According to Bretherton et al (Bretherton et al., 1992), for the long time series, SVD was also superior to CPCA and CCA. This shows that the SVD method can improve the performance of SSTA in describing rainfall.

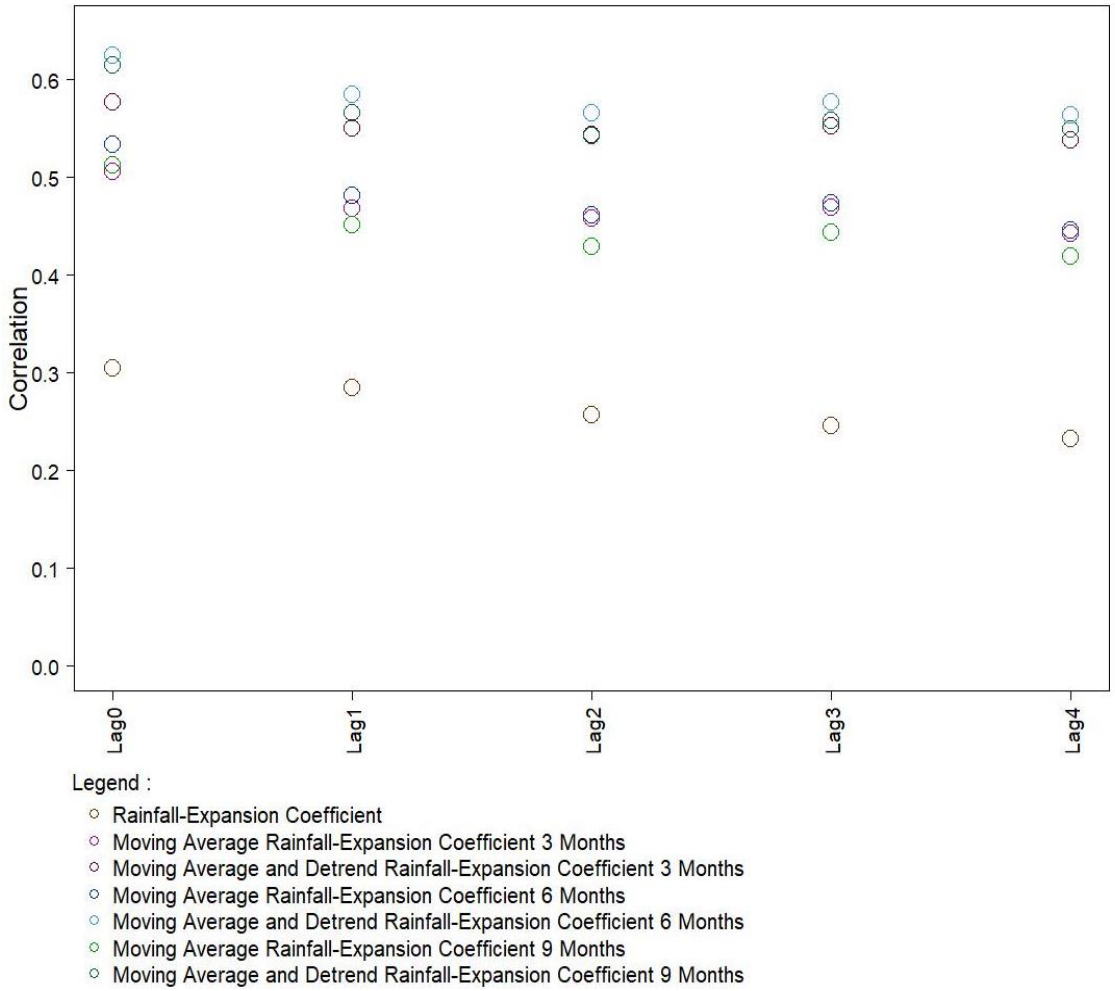

Figure 5. The correlation of rainfall-expansion coefficient, moving average rainfall-expansion, and moving average and detrend rainfall-expansion for 3-, 6- and 9-months.

The correlation coefficient expansion of SSTA in SVD Mode 1 and C12 exhibit similar magnitude but in opposite directions, with inconsistent strengths in each Location of Rain Gauge Stations. Therefore, using expansion coefficients from SSTA in SVD Mode 1 may prove more efficient compared to using them from SVD Mode C12. Furthermore, expansion coefficients in Mode 2 show little correlation to rainfall simulation while expansion coefficients from Mode 1 can strongly impact simulation of rainfall events. Therefore, these findings suggest that expansion coefficients in SVD Mode 1 play an essential role in accurately simulating rainfall while their contribution in Mode 2 was minimal.

Figure 4 presented correlation coefficients of sea surface temperature anomalies (SSTAs) expansion coefficients measured with Standardized Vector Decomposition Mode 1, Mode 2, and C12. Meanwhile, Figure A2 displayed their correlation with rainfall. Figure 4 makes evident how patterns of moving average expansion coefficients vary across modes. Mode 1 generally displays more favorable expansion coefficient patterns compared to Mode 2, though Mode 2 occasionally captures some rainfall-related patterns as well. Mode C12 does not consistently provide more accurate representation than Mode 1, regardless of time scale: 3-month, 6-month and 9-month patterns show similar behavior despite any slight variance from one time scale to the other.

Figure 5 displayed that rainfall and its correlation with sea surface temperature anomalies (SSTAs) expansion coefficient in SVD Mode 1 correlate most strongly at lag 0, while falling off slightly for subsequent lags. This finding aligns with research conducted by (Chhin et al., 2020; Yang and Huang, 2021; Kolstad and MacLeod, 2022) who all found that analyzing SSTA for rainfall simulations without using time lag results in greater fitting power and significance.

Moving average and detrending techniques were applied to the correlation coefficient between SSTA expansion coefficient and rainfall and correlation coefficient, increasing by 0.32 points and 0.1 points respectively. When used over a three-month duration period, moving average and detrended coefficient of SSTA expansion and rainfall reached an incredible correlation of 0.58. As reported by Supari et al. (2018), applying such techniques during peak seasons for rainy and dry seasons can have up to 40% influence on western Java rainfall levels. At six- and nine-month du-

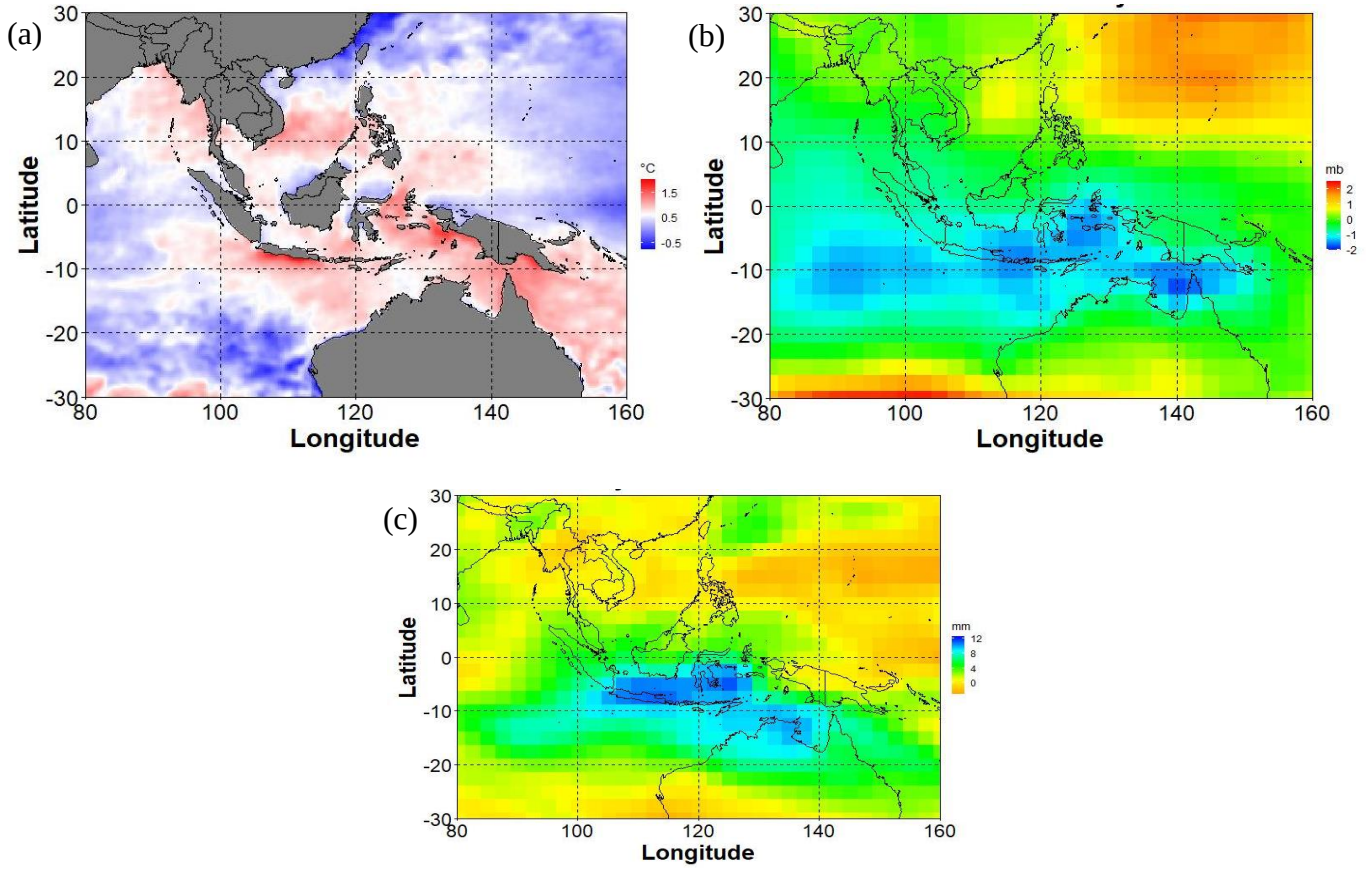

Figure 6. The average of: (a) sea surface temperature anomaly (SSTA), (b) anomaly surface pressure, and (c) anomaly precipitable water content (PWC) from March to October 2010.

rations the correlation coefficient increased to 0.63 and 0.62 respectively, this indicates a relatively close relationship between rainfall and SSTA within this range.

Figure 6 depicted the average sea surface temperature anomaly (SSTA), surface pressure anomaly, and precipitable water content (PWC) anomaly for March through October 2010. During this timeframe, the expansion coefficient for SSTA reached 24.87; during which western Java saw warmer than normal SST conditions than expected as surface air pressure dropped and PWC increased above normal; rainfall also exceeded norm by an impressive amount: 124mm/10 day more rainfall. Lee et al. (2022), reported similar results, characterizing positive SSTA readings in Java and Sumatra waters as the Java Sumatra Nino (JS Nino). This phenomenon induces air movement from the Indian Ocean to the Tropics and influences local rainfall variability.

CONCLUSIONS

This study examines the direct relationship of SSTA with rainfall anomalies in Western Java. In the context of climate dynamics, the process of rainfall formation from SSTA exhibits consistency over longer durations. Studying the relationship between rainfall or SSTA with other elements such as surface air pressure and PWC was interesting to improve the analysis with more precision. The expansion coefficient of SSTA in SVD Mode 1 at lag 0 gives a better performance than SSTA in representing rainfall. This can be seen from the superior correlation value of 0.2 points. However, the spatial pattern of SSTA from SVD has a similar pattern to Pearson's spatial correlation for SSTA with rainfall. Positive anomalies of SSTA in southern Indonesia, east of the Pacific Ocean, and south of Papua New Guinea, while negative anomalies in other regions support the formation of rainfall in western Java. The coefficient of expansion of SSTA within a period of 6-months to 9-months has the best correlation in representing rainfall reaching 0.62 to 0.63. The positive expansion coefficient of SSTA describes SST around the Java Island as being warmer, followed by lower surface pressure and higher the amount of water in the atmosphere than normal and causes higher rainfall in Western Java. This higher rainfall potentially caused the hydrological disaster.

ACKNOWLEDGEMENT

The authors would like to acknowledge the Indonesian Meteorology, Climatology, and Geophysics Agency (BMKG) for their valuable support and provision of meteorological data, which greatly

contributed to the success of this study. Additionally, the authors express their gratitude to IPB University for their collaboration and support, which enhanced the research quality and analysis.

REFERENCES

Aldrian, E., Susanto, R.D., 2003. Identification of three dominant rainfall regions within Indonesia and their relationship to sea surface temperature. International Journal of Climatology 23, 1435–1452. https://doi.org/10.1002/joc.950

Avia, L.Q., 2019. Change in rainfall per-decades over Java Island, Indonesia. IOP Conf. Ser.: Earth Environ. Sci. 374, 012037. https://doi.org/10.1088/1755-1315/374/1/012037

Biasutti, M., 2019. Rainfall trends in the African Sahel: Characteristics, processes, and causes. WIREs Climate Change 10. https://doi.org/10.1002/wcc.591

Bretherton, C.S., 2015. Maximum covariance analysis: Comparing time-dependent spatial fields of data 1–3.

Bretherton, C.S., Smith, C., Wallace, J.M., 1992. An Intercomparison of Methods for Finding Coupled Patterns in Climate Data. Journal of Climate 5, 541–560. https://doi.org/10.1175/1520-0442(1992)005<0541:AIOMFF>2.0.CO;2

Chen, W.T., Hsu, S.P., Tsai, Y.H., Sui, C.H., 2019. The influences of convectively coupled Kelvin waves on multiscale rainfall variability over the South China Sea and maritime continent in December 2016. Journal of Climate 32, 6977–6993. https://doi.org/10.1175/JCLI-D-18-0471.1

Chhin, R., Shwe, M.M., Yoden, S., 2020. Time-lagged correlations associated with interannual variations of pre-monsoon and post-monsoon precipitation in Myanmar and the Indochina Peninsula. International Journal of Climatology 40, 37923812. https://doi.org/10.1002/joc.6428

Huang, B., Liu, C., Banzon, V., Freeman, E., Graham, G., Hankins, B., Smith, T., Zhang, H.M., 2021. Improvements of the Daily Optimum Interpolation Sea Surface Temperature (DOISST) Version 2.1. Journal of Climate 34, 2923–2939. https://doi.org/10.1175/JCLI-D-20-0166.1

Huang, Y., Liu, X., Yin, Z., An, Z., 2021. Global Impact of ENSO on Dust Activities with Emphasis on the Key Region from the Arabian Peninsula to Central Asia. Geophys Res Atmos 126. https://doi.org/10.1029/2020JD034068

Iskandar, I., Lestrai, D.O., Nur, M., 2019. Impact of El Niño and El Niño Modoki Events on Indonesian Rainfall. Makara Journal of Science 23, 217–222. https://doi.org/10.7454/mss.v23i4.11517

Ivanova, D.P., McClean, J.L., Sprintall, J., Chen, R., 2021. The Oceanic Barrier Layer in the Eastern Indian Ocean as a Predictor for Rainfall Over Indonesia and Australia. Geophysical Research Letters 48, 1-12. https://doi.org/10.1029/2021GL094519

Izumo, T., Vialard, J., Lengaigne, M., Suresh, I., 2020. Relevance of Relative Sea Surface Temperature for Tropical Rainfall Interannual Variability. Geophys. Res. Lett. 47. https://doi.org/10.1029/2019GL086182

Jati, M.I.H., Suroso, Santoso, P.B., 2019. Prediction of flood areas using the logistic regression method (case study of the provinces Banten, DKI Jakarta, and West Java). Journal of Physics: Conference Series 1367. https://doi.org/10.1088/17426596/-1367/1/012087

Kolstad, E.W., MacLeod, D., 2022. Lagged oceanic effects on the East African short rains. Climate Dynamics 59, 1043–1056. https://doi.org/10.-1007/s00382-022-06176-6

Lee, H., 2015. General Rainfall Patterns in Indonesia and the Potential Impacts of Local Seas on Rainfall Intensity. Water 7, 1751–1768. https://doi.org/10.-3390/w7041751

Lee, S.K., Lopez, H., FOLTZ, G.R., Lim, E.P., Kim, D., LARSON, S.M., Pujiana, K., VOLKOV, D.L., Chakravorty, S., GOMEZ, F.A., 2022. Java-Sumatra Nino/Nina and Its Impact on Regional Rainfall Variability. Journal of Climate 35, 4291–4308. https://doi.org/10.1175/JCLI-D-21-0616.1

Ma, J., He, W., Chen, Z., Fu, Y., Yin, J., 2020. The impact of north tropical Atlantic sea surface temperature anomalies in the ensuing spring of El Niño on the tropical Indian Ocean and Northwest Pacific. International Journal of Climatology 40, 4978–4991. https://doi.org/10.1002/joc.6500

Makula, E.K., Umutoni, M., Japheth, L., Lipiki, E., Kebacho, L., Tilwebwa, S., 2020. The covariability of sea surface temperature and MAM rainfall on East Africa using singular value decomposition analysis. Geographica Pannonica 24, 261–270. https://doi.org/10.5937/gp24-27577

Nguyen, P.L., Min, S.K., Kim, Y.H., 2021. Combined impacts of the El Niño-Southern Oscillation and Pacific Decadal Oscillation on global droughts assessed using the standardized precipitation evapotranspiration index. International Journal of Climatology 41, E1645–E1662. https://doi.org/10.1002/joc.6796

Nurrohman, F., Tjasyono, B., 2016. Kajian Indeks Stabilitas Atmosfer Terhadap Kejadian Hujan Lebat Di Wilayah Makassar (Studi Kasus Bulan Desember 2013 – 2014). Jurnal Meteorologi

Klimatologi dan Geofisika 3, 18–24. https://doi.-org/10.20961/prosidingsnfa.v3i0.28538

Oueslati, B., Bellon, G., 2015. The double ITCZ bias in CMIP5 models: interaction between SST, large-scale circulation and precipitation. Climate Dynamics 44, 585–607. https://doi.org/10.1007/-s00382-015-2468-6

Reitberger, G., Sauer, T., 2020. Background Subtraction using Adaptive Singular Value Decomposition. J Math Imaging Vis 62, 1159–1172. https://doi.org/10.1007/s10851-020-00967-4

Supari, Tangang, F., Salimun, E., Aldrian, E., Sopaheluwakan, A., Juneng, L., 2018. ENSO modulation of seasonal rainfall and extremes in Indonesia. Climate Dynamics 51, 2559–2580. https://doi.org/10.1007/s00382-017-4028-8

Wati, T., Kusumaningtyas, S.D.A., Aldrian, E., 2019. Study of season onset based on water requirement assessment. IOP Conference Series: Earth and Environmental Science 299. https://doi.org/10.1088/1755-1315/299/1/012042

Wuryanta, A., 2022. Study of ecodrainage system for hydrometeorological disaster mitigation. IOP Conference Series: Earth and Environmental Science 1109. https://doi.org/10.1088/1755-1315/1109/1/012029

Xu, Q., Guan, Z., Jin, D., Hu, D., 2019. Regional characteristics of interannual variability of summer rainfall in the maritime continent and their related anomalous circulation patterns. Journal of Climate 32, 4179–4192. https://doi.org/10.1175/JCLI-D-18-0480.1

Yang, X., Huang, P., 2021. Restored relationship between ENSO and Indian summer monsoon rainfall around 1999/2000. The Innovation 2, 100102. https://doi.org/10.1016/j.xinn.2021.100102

Yu, S.Y., Fan, L., Zhang, Y., Zheng, X.T., Li, Z., 2021. Reexamining the Indian Summer Monsoon Rainfall–ENSO Relationship From Its Recovery in the 21st Century: Role of the Indian Ocean SST Anomaly Associated With Types of ENSO Evolution. Geophysical Research Letters 48. https://doi.org/10.1029/2021GL092873

ANNEX

Figure A1. Spatial pattern of singular value decomposition (SVD) sea surface temperature anomaly (SSTA) mode.

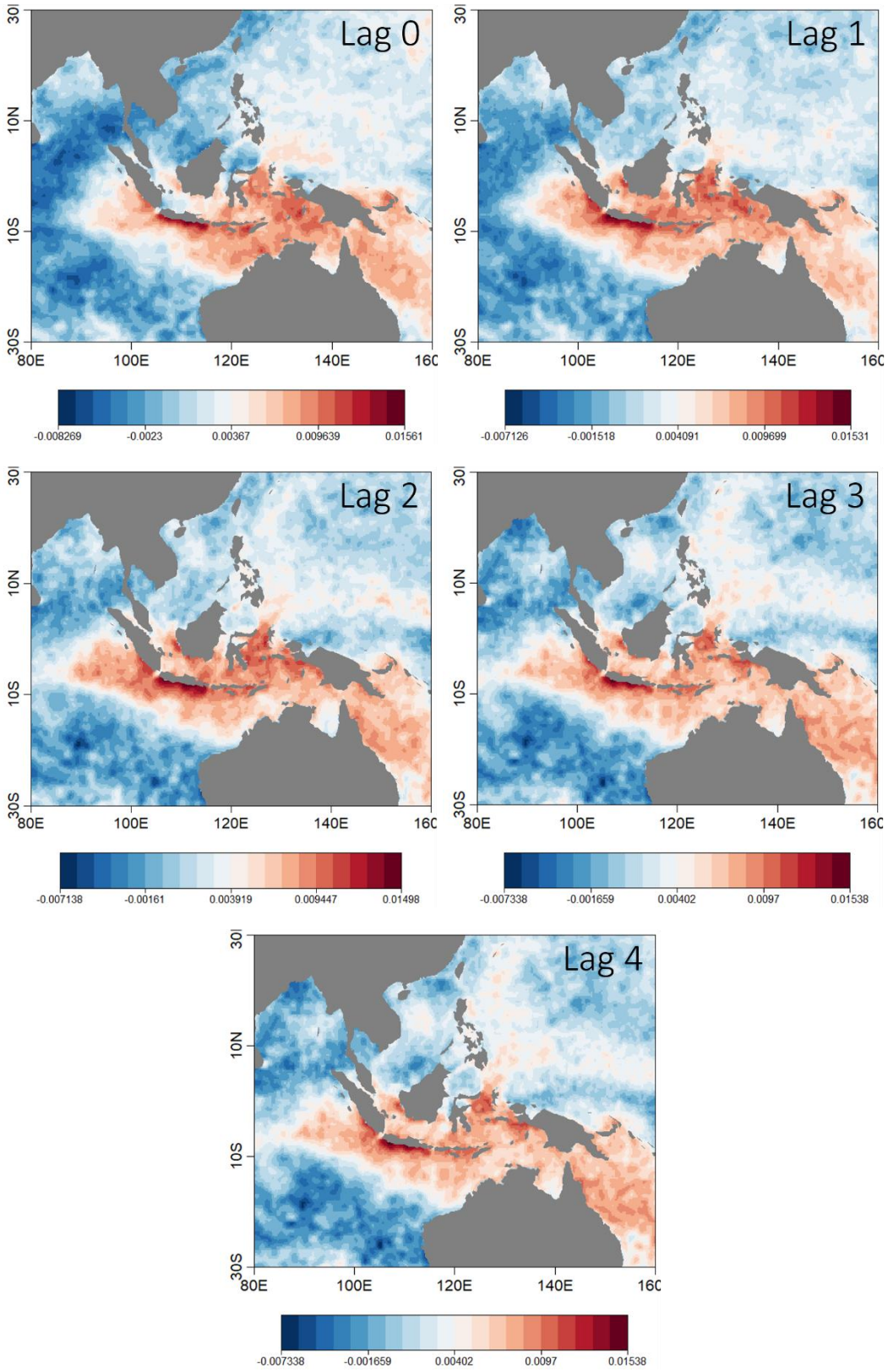

Figure A2. Moving average of standardized 3-months (a) mode 1, (b) mode 2, and (c) mode C12; 6-months (d) mode 1, (e) mode 2, and (f) mode C12; and 9-months (g) mode 1, (h) mode 2, and (i) mode C12 rainfall and expansion coefficient.

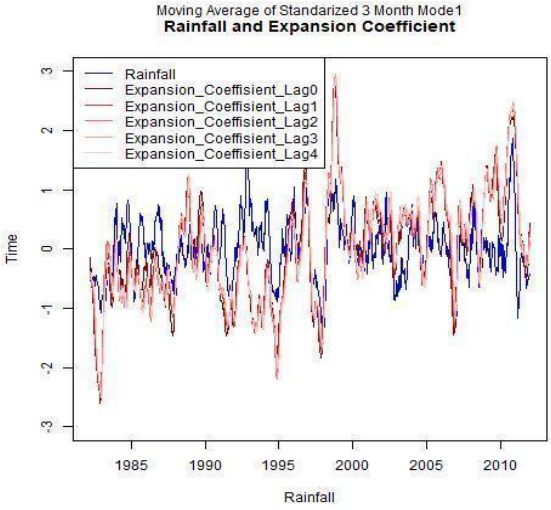

(a)

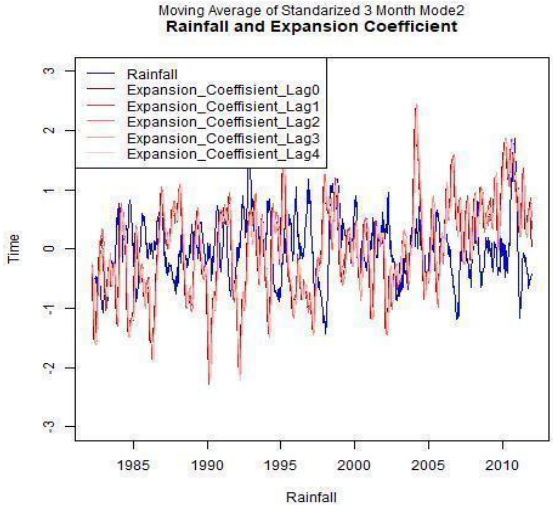

(b)

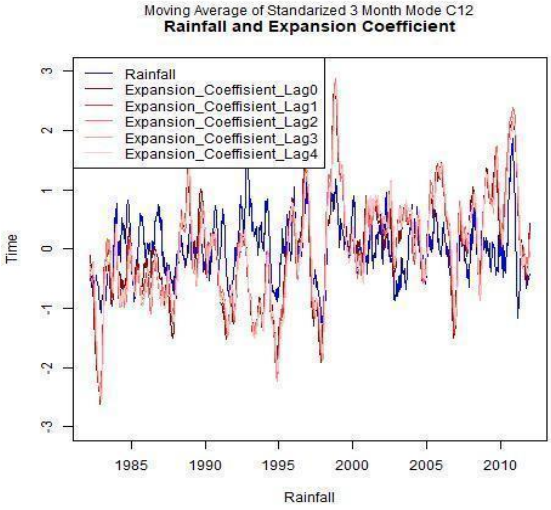

(c)

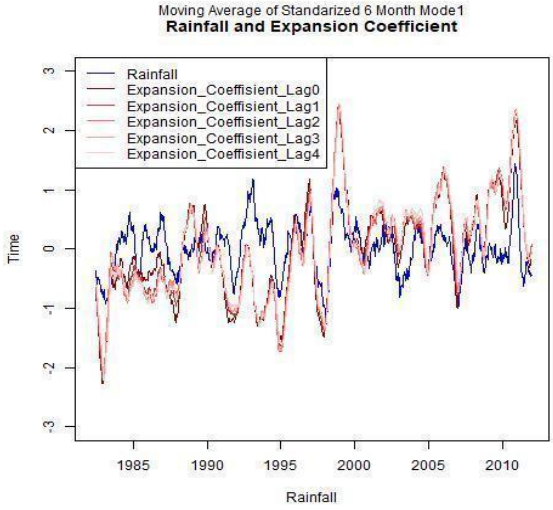

(d)

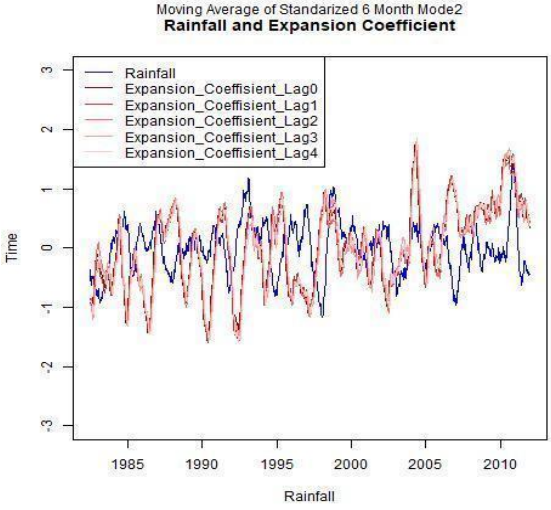

(e)

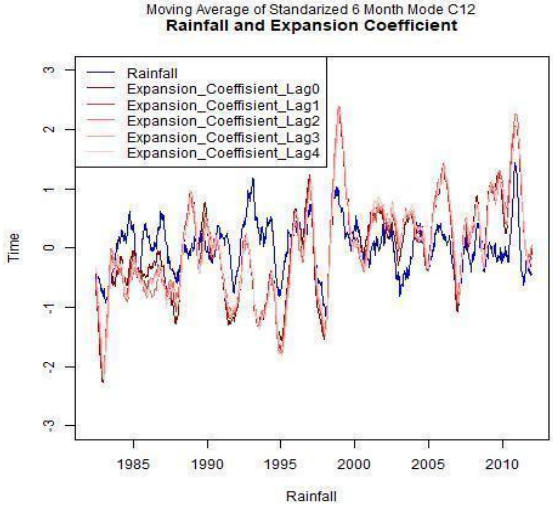

(f)

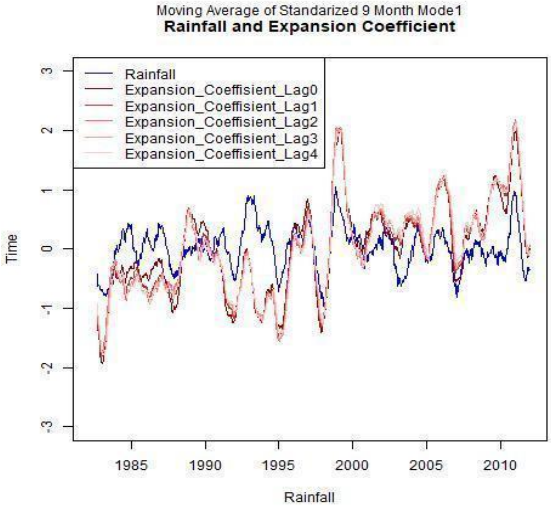
Moving Average of Standarized 9 Month Mode1
Rainfall and Expansion Coefficient
Rainfall
Expansion_Coeffisient_Lag0
Expansion_Coeffisient_Lag1
Expansion_Coeffisient_Lag2
Expansion_Coeffisient_Lag3
Expansion_Coeffisient_Lag4
Time
Rainfall

(g)

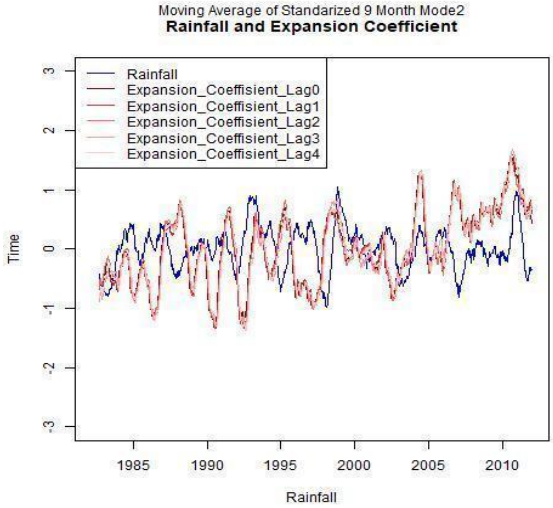
Moving Average of Standarized 9 Month Mode2
Rainfall and Expansion Coefficient
Rainfall
Expansion_Coeffisient_Lag0
Expansion_Coeffisient_Lag1
Expansion_Coeffisient_Lag2
Expansion_Coeffisient_Lag3
Expansion_Coeffisient_Lag4
Time
Rainfall

(h)

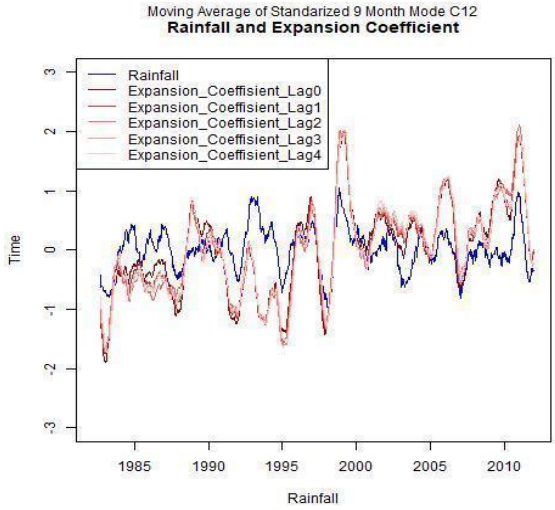
Moving Average of Standarized 9 Month Mode C12
Rainfall and Expansion Coefficient
Rainfall
Expansion_Coeffisient_Lag0
Expansion_Coeffisient_Lag1
Expansion_Coeffisient_Lag2
Expansion_Coeffisient_Lag3
Expansion_Coeffisient_Lag4
Time
Rainfall

(i)